



New precursors for the preparation of pH-sensitive, targeting, and loaded non-porous bridged silsesquioxane nanoparticles

C. Théron, A. Birault, M. Bernhardt, L. M. A. Ali, Cong Tu Nguyen, M. Gary-Bobo, J. Bartlett, M. Wong Chi Man, C. Carcel

► To cite this version:

C. Théron, A. Birault, M. Bernhardt, L. M. A. Ali, Cong Tu Nguyen, et al.. New precursors for the preparation of pH-sensitive, targeting, and loaded non-porous bridged silsesquioxane nanoparticles. Journal of Sol-Gel Science and Technology, 2019, 89 (1), pp.45-55. 10.1007/s10971-018-4676-0 . hal-03095511

HAL Id: hal-03095511

<https://hal.science/hal-03095511>

Submitted on 4 Jan 2021

HAL is a multi-disciplinary open access archive for the deposit and dissemination of scientific research documents, whether they are published or not. The documents may come from teaching and research institutions in France or abroad, or from public or private research centers.

L'archive ouverte pluridisciplinaire **HAL**, est destinée au dépôt et à la diffusion de documents scientifiques de niveau recherche, publiés ou non, émanant des établissements d'enseignement et de recherche français ou étrangers, des laboratoires publics ou privés.

New precursors for the preparation of pH-sensitive, targeting and loaded non-porous bridged silsesquioxane nanoparticles

C. Théron¹, A. Birault^{1,2}, M. Bernhardt¹, L.M.A. Ali³, C. Nguyen³, M. Gary-bobo³, J.R. Bartlett², M. Wong Chi Man¹, C. Carcel^{1*}

[1] ICGM, Univ Montpellier, CNRS, ENSCM, Montpellier, France

[2] Faculty of Science, Health, Education and Engineering, University of the Sunshine Coast, Maroochydore DC, QLD 4558 Australia

[3] Institut des Biomolécules Max Mousseron UMR 5247 CNRS-UM, Faculté de Pharmacie, 15 Avenue Charles Flahault, 34093 Montpellier Cedex 05 (France)

*Corresponding author: carole.carcel@enscm.fr

Highlights

New tetrasilylated precursors with molecular recognition properties were synthesized.

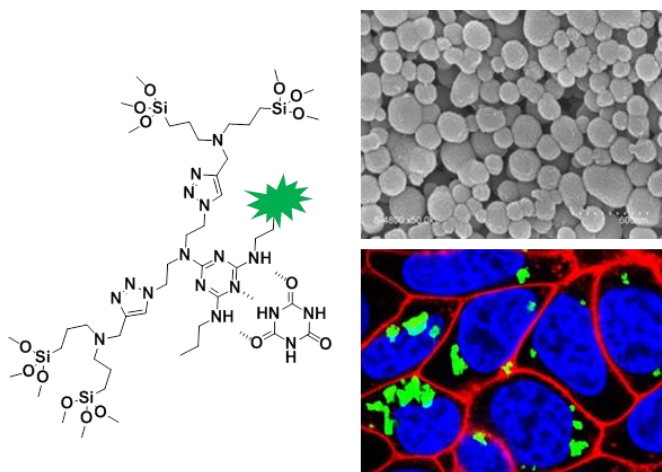
pH-sensitive and loaded non porous bridged silsesquioxane nanoparticles (nano-BS) were prepared.

Nano-BS were internalized into cancer cells.

Abstract: Two new tetrasilylated precursors based on a triazine derivative with molecular recognition properties have been synthesized and are shown to efficiently produce pH-sensitive, targeting and (one step) loaded non-porous bridged silsesquioxane nanoparticles (nano-BS). This was achieved by the sol-gel hydrolysis-condensation of the precursors in the presence of cyanuric acid (CA) H-bonded through the three complementary faces and mimicking 5-fluorouracil (5-FU) anti-cancer drug. The complex in the nano-BS is not affected under neutral medium and operates under acidic conditions to deliver the loaded molecule as demonstrated by FTIR spectroscopic studies. Furthermore, thanks to the presence of the amino function, the nano-BS could be functionalized with targeting or fluorescent systems. Indeed the grafting of fluorescein isothiocyanate revealed the internalization into cancer cells, confirming that nano-BS are promising materials as carriers to avoid side effects of anticancer drug due to a controlled and targeted drug delivery.

Graphical Abstract :

SEM and confocal images of nano-BS



Keywords: Bridged silsesquioxanes nanoparticles / Drug delivery / pH-sensitive / One step drug loading / Targeting.

1. INTRODUCTION

Since the first reports on bridged silsesquioxanes (BS) [1,2] such hybrid materials have attracted much attention due to the complementary properties of the organic and inorganic components with the incorporation of a high level of organic groups regularly and covalently linked to the silica matrix [3,4]. Thus a wide range of properties can be introduced through the organic components, leading to functional BS with applications such as recoverable and recyclable catalysts [5-8], metal-free phosphors in solid-state lighting[9], Eu³⁺-based transparent luminescent solar concentrators [10] and selective extractants for the treatment of acidic aqueous wastes produced by the nuclear industry [11,12]. In addition, the silica matrix is chemically, thermally and mechanically stable and biocompatible [13-15]. The porosity of such materials can also be tailored via selective cleavage of the Si-C bond in the silica matrix [16,17] or by using surfactants to yield periodic mesoporous organosilicates (PMOs) [18,19] in which the bridging organics are located in the walls and can be randomly dispersed [2,3] or ordered. Recently the synthesis of nano-PMOs [20-24] has been achieved and similarly to MSN [25], were also shown to be promising candidates as nano delivery carriers for medical applications [26-30]. It was also shown that the morphology of the material (e.g. hollow or dense spheres) [26] as well as the organic functions within the walls (compared with functionalized MSN) [27] could improve or affect their drug release properties. Nevertheless, the use of nano-PMOs in the medical field is still at a very early stage of development compared to the facile, wide-spread synthesis of MSN with pure Si-O composition [31]. In particular, the size [32], wettability, electrostatic charge and chemical properties of the bridging organic units of the precursors can affect the cooperative self-assembly of surfactant species and organosilica source and disrupt the formation of monodispersed and mesoporous NPs. Thus, it is necessary to choose the appropriate synthesis strategy and experimental parameters to control the reaction kinetics in order to prepare NPs with the desired size, porosity and structures.

We recently reported a new approach for designing BS-based drug carriers, involving the sol-gel processing of a triazine-based organosilane precursor in the presence of a non-silylated 5-FU molecule [33], held by weak H-bonding interactions in the resulting bulk material. The 5-FU acted both as the templating agent and also as an active anti-cancer drug. No release of the drug was observed from the BS at neutral pH but release was achieved at mildly acidic pH such as that found in lysosomes. This first study confirmed the strategy of developing well-designed bridged silsesquioxanes as hybrid materials for biomedical applications such as drug-delivery, since they obviously comply with the required conditions for

therapeutic applications, namely a non-premature release and controlled-release triggered by an environmental stimulus. In addition, compared to other MSN nanocarriers, they allow a direct loading of drugs (one step) during the synthesis. However, one of the key requirements of drug delivery vectors for *in vitro* or *in vivo* applications is the control of their particle size, with particles smaller than 300 nm required for efficient cellular uptake. The control of particle size is mainly governed by the synthesis method and specific experimental parameters employed, and as mentioned previously, the presence of bulky organic groups often militates against the formation of nanoparticles. Indeed, earlier reported attempts to obtain nano-BS using a bis-silylated triazine-based organosilane precursor were unsuccessful [34].

To date, only a few reports describing the synthesis of nano-BS from organosilane precursors containing large bridging organic unit have appeared. In these recently-published studies, polysilylated precursors [35-37] alone or co-condensation with another bridged organosilane [38,39] were used and increasing the number of trialkoxysilyl groups proved to be beneficial for producing nanoparticles. Herein we describe the synthesis of a new nano-BS carrier with an appropriate size for passive targeting of cancer cells, using a surfactant-free method under neutral condition and cyanuric acid as a model compound to mimic the 5-FU drug. To achieve this, a new tetrasilylated triazine-based precursor (**7**) was initially designed and studied. Then an amino function was introduced on the triazine motif to obtain a new precursor (**8**). Post-functionalization of the resulting nanoparticles with a fluorescent probe for imaging was performed, to enable the internalization of the nano-BS inside tumor cells to be investigated.

2. EXPERIMENTAL PROCEDURE

2.1 General methods

All reagents were used as received. Solvents were dried by using a MB SPS-800 apparatus. FTIR spectra were obtained using a PerkinElmer Spectrum BX spectrophotometer equipped with GladiaATR. Liquid ¹H and ¹³C NMR spectra were recorded on a Bruker AC-400 spectrometer at room temperature with CDCl₃ as solvent and tetramethylsilane (TMS) as an internal reference. High-resolution mass spectra (Q-TOF ES+) were measured on a JEOL MS-DX 300 mass spectrometer.

2.2 Precursor synthesis

1 [40]: A solution of bis-(2-chloro-ethyl)-amine hydrochloride (1.8 g, 10 mmol) and sodium azide (3.3 g, 50 mmol) in water (50 mL) was heated at 80 °C for 24 h. After evaporating most of the water, the solution was treated with NaOH (1 M, 30 mL) and then extracted with diethyl ether. The organic layer was washed with H₂O and dried over MgSO₄. Finally, the solvent was removed under reduced pressure to afford **1** as a colorless oil in 70% yield, which was used without further purification. ¹H NMR (CDCl₃, 400MHz): δ = 1.39 (s, 1H); 2.70 (t, 4H); 3.29 (t, 4H). ¹³C NMR (CDCl₃, 100MHz): δ = 47.68 (s); 50.90 (s). HRMS (ESI+): m/z: calcd for C₄H₁₀N₇ (M+H): 156.0998; found: 156.1000.

2: 2,4,6-Trichloro-1,3,5-triazine (0.775 g, 3.82 mmol) was dissolved in THF (15 mL) and the solution was cooled in a water/ice bath before adding diisopropylethylamine (1 mL, 5.73 mmol). Then, **1** (0.593 g, 3.82 mmol) dissolved in THF (15 mL) was added dropwise under magnetic stirring which was continued for 2 h after addition at 0°C. After warming to room

temperature, THF was removed under reduced pressure. The residue was dissolved in CH₂Cl₂ and washed with 1 M HCl. The organic layer was washed with H₂O and dried over MgSO₄. The solvent was removed under reduced pressure and the resulting solid was purified by column chromatography (SiO₂; CH₂Cl₂) to afford **2** as a beige solid in 66% yield. ¹H NMR (CDCl₃, 400MHz): δ = 3.61 (t, 4H); 3.81 (t, 4H). ¹³C NMR (CDCl₃, 100MHz): δ = 48.45 (s); 48.91 (s); 165.02 (s); 170.39 (s). HRMS (ESI+): m/z: calcd for C₇H₉Cl₂N₁₀ (M+H): 303.0389; found: 303.0387.

3: Propylamine (2.1 mL, 25.4 mmol) and **2** (0.77 g, 2.54 mmol) were refluxed in THF (30 mL) overnight. After concentrating under reduced pressure, the resulting oil was dissolved in CH₂Cl₂. The organic layer was washed with H₂O and dried over MgSO₄. The solvent was removed under vacuum and the resulting solid was purified by column chromatography (SiO₂; CH₂Cl₂ then CH₂Cl₂/MeOH 10/0.25) to afford **3** as a colorless oil in 90% yield. ¹H NMR (CDCl₃, 400MHz): δ = 0.93 (t, 6H); 1.55 (m, 4H); 3.28 (t, 4H); 3.52 (t, 4H); 3.70 (t, 4H); 4.84 (s, 2H). ¹³C NMR (CDCl₃, 100MHz): δ = 11.43 (s); 23.06 (s); 42.50 (s); 47.65 (s); 49.75 (s); 165.07 (s); 165.81 (s). HRMS (ESI+): m/z: calcd for C₁₃H₂₅N₁₂ (M+H): 349.2325; found: 349.2319.

4: To a solution of **2** (0.61 g, 2.0 mmol) in THF (75 mL) was added dropwise successively DIPEA (0.52 mL, 3.0 mmol) and propylamine (0.164 mL, 2.0 mmol). The resulting solution was then stirred overnight at 25°C. THF was removed under reduced pressure. The residue was dissolved in CH₂Cl₂ and washed with 1 M HCl. The organic layer was washed with H₂O and dried over MgSO₄. The solvent was removed under reduced pressure and the resulting solid was purified by column chromatography (SiO₂; CH₂Cl₂/Cyclohexane 80/20) to afford **4** as a white powder in 85% yield. ¹H NMR (CDCl₃, 400MHz): δ = 0.97 (t, 3H); 1.59 (m, 2H); 3.33 (t, 2H); 3.58 (t, 4H); 3.75 (t, 4H). ¹³C NMR (CDCl₃, 100MHz): δ = 11.32 (s); 22.55 (s); 42.78 (s); 49.01 (s); 49.83 (s); 164.99 (s); 165.46 (s); 168.54 (s). HRMS (ESI+): m/z: calcd for C₁₀H₁₇ClN₁₁ (M+H): 326.1357; found: 326.1347.

5: A solution of **4** (0.282 g, 0.866 mmol) in THF (35 mL) was heated at 55°C for 10 min before adding dropwise ethylenediamine (0.56 mL, 8.66 mmol). The solution was then refluxed overnight. After concentrating under reduced pressure, the resulting oil was dissolved in CH₂Cl₂. The organic layer was washed with H₂O and dried over MgSO₄. The solvent was removed under reduced pressure and the resulting solid was purified by column chromatography (SiO₂; CH₂Cl₂ then CH₂Cl₂/MeOH/NH₄OH 80/1/0.25) to afford **5** as white powder in 85% yield. ¹H NMR (CDCl₃, 400MHz): δ = 0.93 (t, 3H); 1.55 (m, 2H); 2.86 (m, 2H); 3.27 (t, 2H); 3.40 (t, 2H); 3.51 (t, 4H); 3.70 (t, 4H). ¹³C NMR (CDCl₃, 100MHz): δ = 11.46 (s); 23.04 (s); 41.64 (s); 42.42 (s); 43.24 (s); 47.59 (s); 49.68 (s); 165.03 (s); 166.12 (s). HRMS (ESI+): m/z: calcd for C₁₂H₂₄N₁₃ (M+H): 350.2278; found: 350.2252.

6: This compound was synthesized according to a previously reported procedure [41,42]. To a solution of bis(3-(triethoxysilyl)-propyl)amine (21.4 g, 50.2 mmol) in THF (250 mL) with 1000 ppm of water (250 μL) was added calcium hydride (5.6 g, 133.0 mmol) and propargyl bromide (80% in toluene, 8.5 mL, 95.4 mmol). The solution was stirred for 18 h at room temperature. Solvents were removed under reduced pressure and the crude product was extracted with pentane giving a yellow oil. After purification by distillation (130°C / 2x10⁻³ mbar), **6** was obtained as a colorless oil with 85% yield. ¹H NMR (CDCl₃, 400 MHz): δ = 0.59 (t, 4H); 1.20 (t, 18H);

1.54 (m, 4H); 2.12 (s, 1H); 2.46 (t, 4H); 3.37 (d, 2H); 3.78 (q, 12H). ^{13}C NMR (CDCl_3 , 100MHz): δ = 7.80 (s); 18.14 (s); 20.69 (s); 41.65 (s); 56.41 (s); 58.16 (s); 72.28 (s); 78.78 (s). HRMS (ESI+): m/z : calcd for $\text{C}_{21}\text{H}_{46}\text{NO}_6\text{Si}_2$ (M+H): 464.2864; found: 464.2873.

7: A microwave tube was filled under nitrogen with **6** (1.51 g, 3.25 mmol), **3** (0.566 g, 1.62 mmol), $[\text{CuBr}(\text{PPh}_3)_3]$ (38 mg, 0.041 mmol), dry triethylamine (1 mL) and dry THF (1 mL) then sealed. After 20 minutes under microwave irradiation at 100 °C (maximum power = 200 W), the reaction mixture was cooled, then the solvents were removed under vacuum. After addition of dry pentane, the mixture was filtered and the filtrate was concentrated to afford **7** as a yellow oil with a quantitative yield and was used without further purification. ^1H NMR (CDCl_3 , 400MHz): δ = 0.55 (t, 8H); 0.95 (t, 6H); 1.20 (t, 36H); 1.58 (m, 12H); 2.39 (t, 8H); 3.28 (q, 4H); 3.66 (m, 8H); 3.79 (q, 24H); 4.49 (t, 4H); 7.32 (s, 2H). ^{13}C NMR (CDCl_3 , 100MHz): δ = 7.86 (s); 11.50 (s); 18.28 (s); 20.26 (s); 23.05 (s); 42.47 (s); 45.90 (s); 48.16 (s); 48.60 (s); 56.46 (s); 58.29 (s); 123.11 (s); 128.51 (s); 132.01 (s). HRMS (ESI+): m/z : calcd for $\text{C}_{55}\text{H}_{115}\text{N}_{14}\text{O}_{12}\text{Si}_4$ (M+H): 1275.7896; found: 1275.7910.

8: A microwave tube was filled under nitrogen with **6** (1.95 g, 4.22 mmol), **5** (0.736 g, 2.11 mmol), $[\text{CuBr}(\text{PPh}_3)_3]$ (49 mg, 0.053 mmol), dry triethylamine (1.5 mL) and dry THF (1.5 mL) and then sealed. After 20 minutes under microwave irradiation at 100 °C (maximum power = 200 W), the reaction mixture was cooled, then the solvents were removed under vacuum. After addition of dry pentane, the mixture was filtered and the filtrate was concentrated to afford **8** as a yellow oil with a quantitative yield and was used without further purification. ^1H NMR (CDCl_3 , 400MHz): δ = 0.55 (t, 8H); 0.91 (t, 3H); 1.13 (t, 36H); 1.45 (m, 10H); 2.26 (t, 8H); 2.39 (t, 2H); 3.15 (q, 2H); 3.62 (m, 10H); 3.72 (q, 24H); 4.45 (t, 4H); 7.85 (s, 2H). ^{13}C NMR (CDCl_3 , 100MHz): δ = 7.35; 11.69; 18.12; 20.47; 25.15; 41.83; 45.73; 47.58; 55.51; 57.61; 67.03; 123.69; 128.64; 164.60; 165.56. HRMS (ESI+): m/z : calcd for $\text{C}_{54}\text{H}_{114}\text{N}_{15}\text{O}_{12}\text{Si}_4$ (M+H): 1276.7849; found: 1276.7883.

2.3 Materials

M0T series: In a vial, compound **7** or **8** (1eq) was completely dissolved in DMSO (300 mM or 20 mM) at 50 °C. After 1 h, water (24 eq) and NH_4F (0.04 eq, 0.25 M solution) were added. For the 300 mM system, a white gel was spontaneously formed, whereas for the 20 mM system, a precipitate was observed after a few hours. The vial was left under static conditions at room temperature for 3 days. After successive washing with water, ethanol, and acetone, a white powder was obtained. **M0T** : **7** (300 mM) ; **M0TA** : **8** (20 mM)

M1T series: In a vial, compound **7** or **8** (1 eq) and CA (0.33 eq) were completely dissolved in DMSO (300 mM, 100 mM, 50 mM or 20 mM) at 50 °C. After 1 h, water (24 eq) and NH_4F (0.04 eq, 0.25 M solution) were added. For the 300 mM system, a white gel was spontaneously formed, whereas for the others concentrations, a precipitate was observed after a few hours. The vial was left under static conditions at room temperature for 3 days. After successive washing with water, ethanol, and acetone, a white powder was obtained. **M1T**: **7** (300 mM)+CA; **M1T2**: **7** (100 mM)+CA; **M1T3**: **7** (50 mM)+CA; **M1T4**: **7** (20 mM)+CA ; **M1TA**: **8** (20 mM)+CA

M2T series: **M1T** or **M1TA** (50 mg) was suspended in EtOH (10 mL) with HCl (9 μL , 10^{-2} M) and heated under reflux with stirring for 24 h. The resulting solid was filtered and washed

several times with ethanol, yielding a white powder. Finally, it was treated with aqueous NEt_3 (5 mL of water, 0.5 mL of NEt_3) and stirred overnight to neutralize the protonated amine. **M2T** materials were obtained as white powders after drying.

M3T series: **M1T**, **M1T4** or **M1TA** (50 mg) was suspended in EtOH (20 mL) and heated under reflux with stirring for 24 h. The resulting solid was filtered and washed several times with ethanol, yielding a white powder. **M3T series** were obtained as white powders after drying.

M1TAF: In a vial, **M1TA** (5 mg) was suspended in absolute EtOH (5 mL) before adding FITC (3.5 mg, excess). The suspension was stirred (600 rpm) in the dark for 24 h at 25°C. The resulting powders were washed 4 times with absolute EtOH (20 min, 10000 rpm) to afford **M1TAF**.

2.4 Biological analyses

Cell culture. Human breast (MCF-7) and colorectal (HCT-116) cancer cells were purchased from ATCC (American Type Culture Collection, Manassas, VA). MCF-7 cells were cultured in Dulbecco's Modified Eagle's Medium (DMEM-F12) supplemented with 10% foetal bovine serum and antibiotics (100 U.mL^{-1} penicillin and 100 $\mu\text{g.mL}^{-1}$ streptomycin). HCT-116 cells were cultured in McCoy's 5A Medium supplemented with 10% foetal bovine serum and antibiotics (100 U.mL^{-1} penicillin and 100 $\mu\text{g.mL}^{-1}$ streptomycin). These cells were grown in humidified atmosphere at 37 °C under 5% CO_2 .

Cellular uptake. The cellular uptake experiment was performed using confocal fluorescence microscopy on living cells. MCF-7 and HCT-116 cells were plated onto Lab-Tek II Chambered Coverglass (Nalge Nunc International Ref 155382) in 0.5 mL culture medium for 24 h. Then, human cancer cells were treated with 20 $\mu\text{g.mL}^{-1}$ of fluorescent nanoparticles conjugated with FITC (**M1TAF**) for 24 h. Fifteen minutes before the end of incubation, cells were loaded with CellMaskTM Orange plasma membrane stain (Invitrogen, Cergy Pontoise, France, C10045) for membrane staining at a final concentration of 5 $\mu\text{g.mL}^{-1}$. At the same time, nuclei were stained with Hoechst 33342 at a final concentration of 5 $\mu\text{g.mL}^{-1}$. Then cells were washed two times with culture medium. Confocal fluorescence microscopy was performed on living cells under a 488 nm wavelength excitation for nanoparticles, 750 nm for nuclei and 561 nm for cell membranes.

3. RESULTS AND DISCUSSION

3.1. Synthesis of the tetrasilylated triazine precursors

The preparation of the new BS precursors (Fig. 1) involved reacting the bis-silylated propargylamine **6** [41,42] with compound **A**, based on a triazine moiety bearing two azide functions, with a "donor-acceptor-donor" (DAD) molecular recognition motif. The CuAAC "Click" coupling of these compounds led to the tetrasilylated precursors (**7** and **8**) with the desired molecular recognition pattern and $\text{R} = \text{CH}_3$ or NH_2 , respectively.

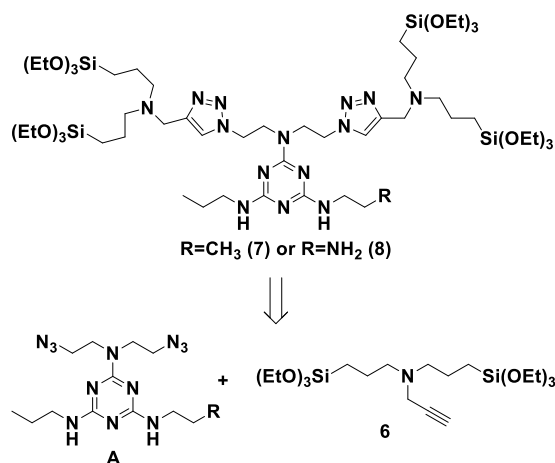


Fig. 1 Pathway for the new precursors (**7** or **8**) synthesis.

1 (Fig. 2) was prepared as described in the literature[40] by mixing sodium azide with bis-(2-chloroethyl) amine in water at 80 °C for 24 h. Compound **1** was added dropwise to a solution of cyanuric chloride in THF in the presence of DIPEA at 0 °C. Purification on a silica column afforded **2** in 66% yield. Then **2** was dissolved in THF with either 10 equivalents of propylamine under reflux or 1 equivalent of propylamine at room temperature to give, after washing and purification, **3** or **4**, respectively in 90% and 85% yield. **4** was then stirred in refluxing THF overnight in the presence of a very large excess of ethylenediamine to give, after purification, **5** in 85% yield. This new compound is di-symmetrically substituted at the level of the DAD unit with functionalization on one side by a propyl group and on the other side by a primary amine.

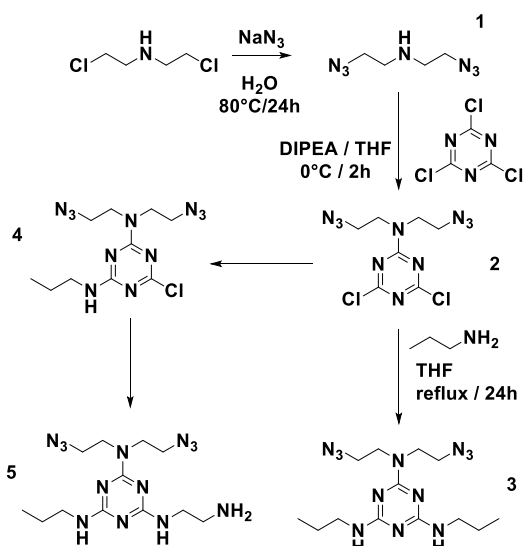


Fig. 2 Synthesis of the triazine derivatives **3** and **5**.

As mentioned before, fragment **6** (Fig. 3) was synthesized according to the literature using CaH₂, propargyl bromide and bis (triethoxysilylpropyl) amine in THF with a small quantity of water under stirring for 18 h at room temperature [41,42]. After washing with pentane, **6** is obtained with a yield of 85% by distillation under reduced pressure. The last step to obtain the tetrasilyl precursors is click coupling between **6** and either **3** or **5**. The reagents are introduced into a microwave tube in the presence of the copper catalyst and NEt₃ in THF. The tube is placed in the microwave apparatus at 100 °C for 20 minutes. After the reaction was complete, the solution was transferred to a Schlenk tube and the solvents were evaporated under reduced

pressure. **7** and **8** were obtained in quantitative yield without purification.

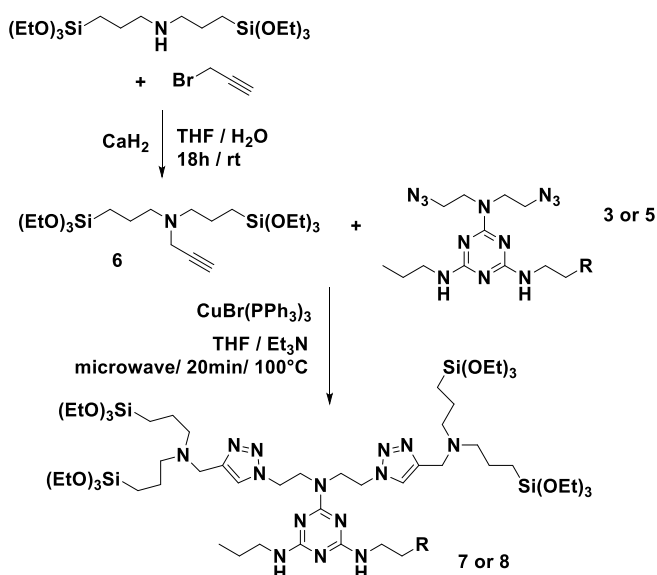


Fig. 3 Synthesis of fragment **6** and Click coupling.

3.2 Complex formation in solution

The complex formation between the precursors and cyanuric acid as template was studied by ¹H liquid NMR (Fig. 4), focusing on the NH proton of cyanuric acid (CA) at around 11 ppm.

Fig 4 shows four spectra all obtained in DMSO-D₆ as solvent corresponding (from bottom to top) respectively to pure CA, a 1:1 molar ratio of CA with **7**, a 1:3 molar ratio of CA with **7** and finally pure **7**. For pure CA, the spectrum shows a single narrow peak at 11.15 ppm while the addition of an equimolar amount of **7** in the same tube results in a broadening of this peak centred at 11.12 ppm. After the subsequent addition of an additional two equivalents of **7** to reach the ideal stoichiometric proportion of the complex (1:3 of CA: **7**), the intensity of the broad peak decreases with a slight shift to 11.01 ppm. These data demonstrate the H-bonds formation confirming the presence of the complex in solution as already observed with the related bis-silylated precursor reported earlier[33].

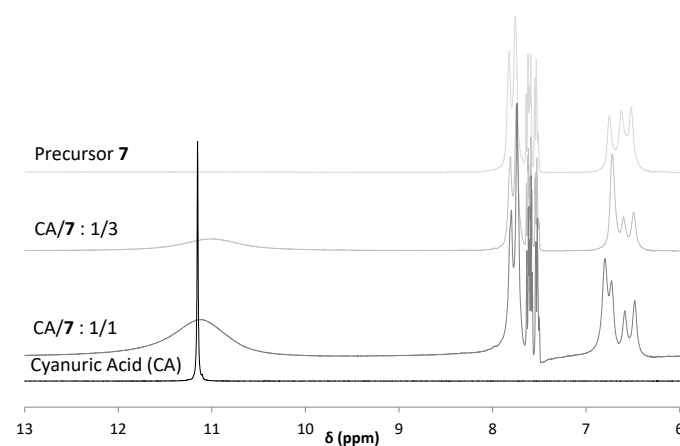


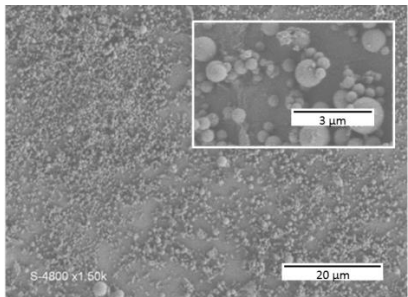
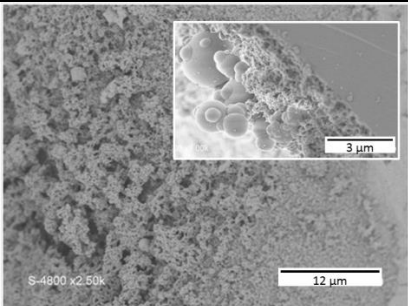
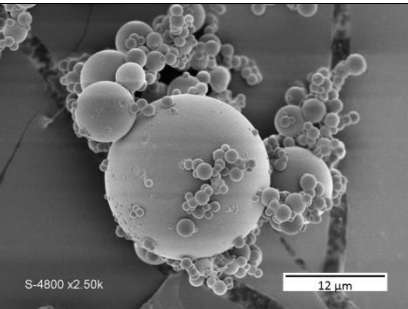
Fig. 4 Liquid ¹H NMR study of the interaction between **7** and CA

3.3 Nanoparticles preparation

We performed the hydrolysis-condensation reactions from a mixture of three molar equivalents of **7** and one molar equivalent of CA in hot DMSO (T = 50 °C) to which 24 molar equivalents

of water were added (two equivalents per ethoxy group) and 0.04 molar equivalent of NH_4F as nucleophilic catalyst (1 mol% per atom of silicon). The mixture was then left under static conditions at room temperature for 3 days. After successive washing with water, ethanol and acetone, a white powder was obtained by centrifugation. Finally, the materials were dried under vacuum at 80 °C to remove traces of solvent. At the same time, the corresponding "reference" materials without CA were prepared under the same conditions. In order to determine the optimal conditions to obtain nanoparticles, several experiments were performed in parallel at different concentrations of **7** in DMSO (300 mM, 100 mM, 50 mM and 20 mM).

For the higher concentration (300 mM), a gel formed almost instantaneously. For the other three concentrations, no gel was observed after the addition of the catalyst, with precipitation occurring instead. These materials were then studied by scanning electron microscopy to investigate their morphologies (Table 1).

SEM images	Name
	Precursor / concentration
	AC
	Gelation
	Precipitation
	M0T
	7/300 mM
	No
	M1T
	7/300 mM
	Yes
	Observed after 10 min
	M1T2
	7/100 mM
	Yes
	No
	M1T3
	7/50 mM

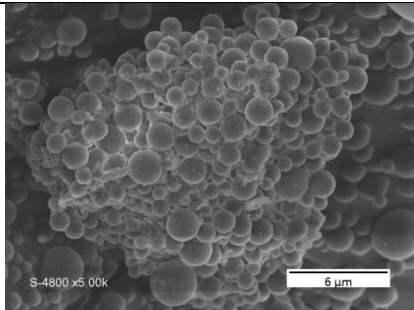
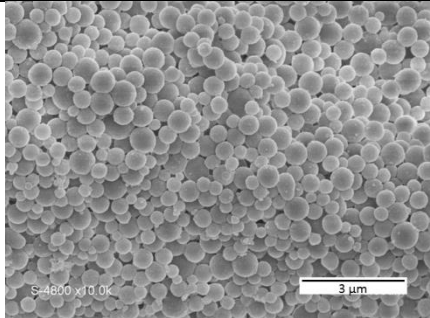
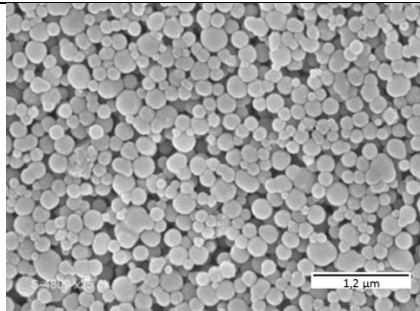
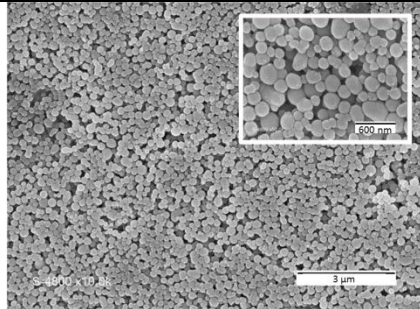
	Yes
	No
	Observed after several hours
	M1T4
	7/20 mM
	Yes
	No
	M0TA
	8/20 mM
	No
	M1TA
	8/20 mM
	Yes
	No
	Observed after several hours

Table 1 SEM pictures of all materials

M0T, prepared without CA, showed a spherical morphology with a relatively homogeneous size distribution. The majority of particles exhibited dimension within the range of 300 to 600 nm, with small quantities of other spherical particles with diameters up to 1.5 μm. The micrographs of **M1T** containing CA, revealed a change in morphology with a fibrous morphology connecting spherical particles being evident. Agglomerated spherical particles were also evident in this case, with a size distribution ranging from 0.5 to 3 μm. Diluting the precursor concentration in DMSO by a factor of two led to spherical particles corresponding to **M1T2**. However, these particles are very large and exhibited a heterogeneous size distribution ranging from around 1 to 15 μm. A further two-fold decrease in reactant concentration gave **M1T3**, with finer particles exhibiting sizes between 1 and 2 μm. Decreasing the concentration of **7** down to 20 mM resulted in **M1T4**, which exhibited a much narrower size distribution between 400 and 600 nm, close to the desired size of 300 nm. Thus dilution favours the formation of nanoparticles.

We next considered the preparation of nanoparticles with **8** under the same conditions as **M1T4**. SEM images of the corresponding material, **M1TA**, showed spherical particles with a size distribution within the range of 90 to 230 nm. TEM images confirmed this size range and revealed the dense character of the spherical nanoparticles (Fig. 5). In parallel, a reference sample was also prepared without CA (**M0TA**) and in this case, SEM images also revealed particles with sizes smaller than 300 nm.

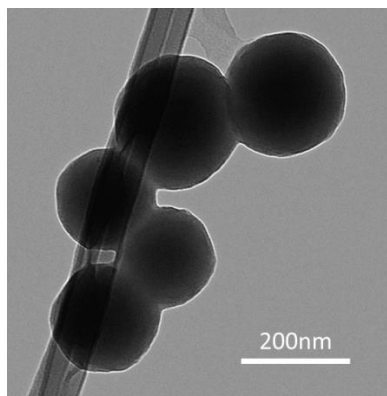


Fig. 5 TEM image of **M1TA**

3.4 Complex stability and release of CA

The stability of these new systems under neutral condition and their ability to release the template compound CA were studied and monitored by IR, first on the bulk material and then on nano-BS.

The stability of the complex in **M1T** was investigated by refluxing a suspension in EtOH for 24 h. The resulting **M3T** was then recovered by centrifugation and washed successively with water, ethanol and acetone before drying. In order to remove CA from **M1T**, the latter was also suspended in a solution of HCl in ethanol (10^{-2} M). After stirring overnight under reflux and after consecutive washings and centrifugation with water, ethanol and acetone, a material expected to be free of CA was obtained. In order to regenerate the complexation sites by deprotonating the triazine, this material was placed in distilled water in the presence of Et_3N and vigorously stirring for 12 h. The material **M2T** was then recovered after washing and centrifugation with water, ethanol and acetone. Fig. 6 shows the different IR spectra obtained from this new series of materials. CA exhibits a characteristic $\text{C}=\text{O}$ vibration at 1720 cm^{-1} which can be employed to detect the presence or absence of CA in the materials. Indeed, this band is absent in **7** and **M0T** but visible in the case of **M1T**. Despite the treatment in refluxing EtOH, this band is still visible for **M3T**, confirming the stability of the complex. Conversely, its disappearance was observed for **M2T** after the acidic treatment, demonstrating the efficiency of the latter in cleaving the hydrogen bonds of the complex, which results in the release of CA.

From the nano-BS **M1T4** and **M1TA**, the presence of CA after washing as well as the stability of the complex after refluxing in ethanol (**M3T4** and **M3TA**) were also monitored by IR spectroscopy (Fig. 7 and 8), via the characteristic band of CA in its complexed form with the precursors at 1720 cm^{-1} . The IR data reveal that cyanuric acid is also released from the nano-BS, since in **M2T4** and **M2TA** the band at 1720 cm^{-1} completely disappeared.

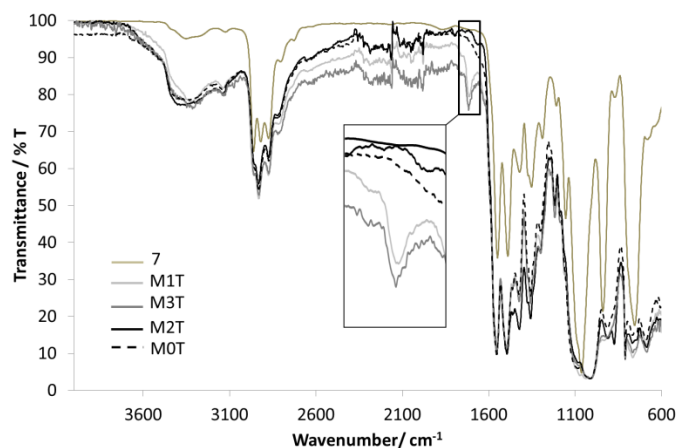


Fig. 6 : IR spectra of bulk materials obtained from **7**

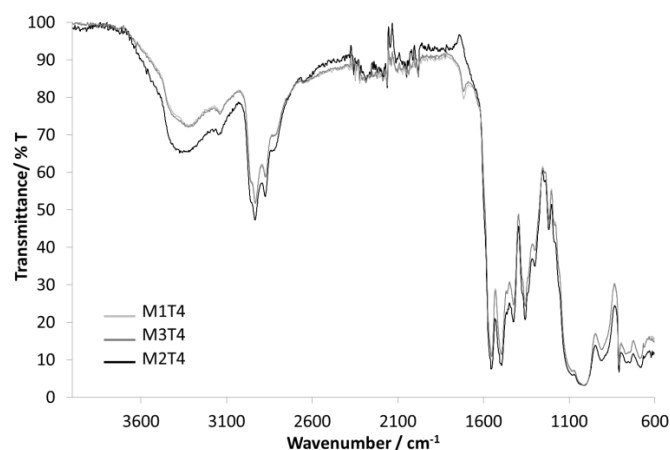


Fig. 7 IR spectra of nanoparticles obtained from **7**

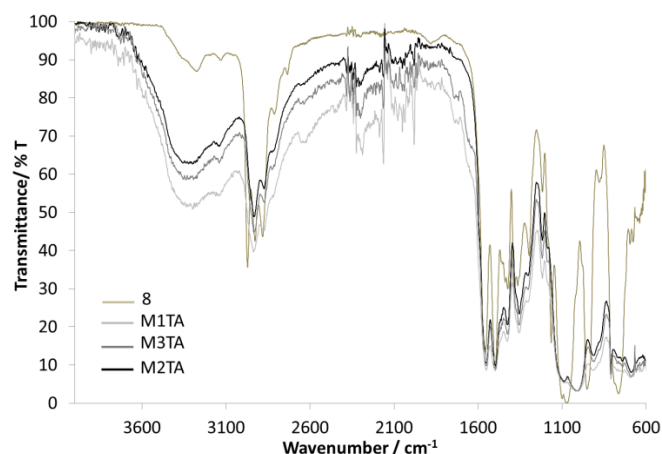


Fig. 8 IR spectra of nanoparticles obtained from **8**

3.5 Nanoparticle functionalization and internalization in cancer cells

Due to the amino function of **8**, the nano-BS **M1TA** could be further functionalized with specific targeting molecules or fluorescent probes. In this study, fluorescein isothiocyanate (FITC) was grafted onto the nanoparticles, which enabled their uptake in cancer cells to be monitored. Grafting was achieved by suspending **M1TA** in EtOH with an excess of FITC, and stirring the resulting mixture in the dark for 24 h to afford **M1TAF** after washing and drying (Fig. 9A).

The passive targeting and internalization potential of these nanoparticles were then studied on cancer cells. Two different human cancer cell lines were used and incubated with

fluorescent nanoparticles (**M1ATF**) at a concentration of $20\ \mu\text{g}\cdot\text{mL}^{-1}$ for 24 h. The nuclei of living cells were stained in blue with Hoechst 33342, cell membranes were stained in red with orange CellMask™ and **M1TAF** grafted with FITC appeared in green. Fig. 9 shows that **M1TAF** nanoparticles are efficiently internalized into breast (MCF-7) and colorectal (HCT-116) cancer cells. This demonstrates the potential of such material to target and treat cancer.

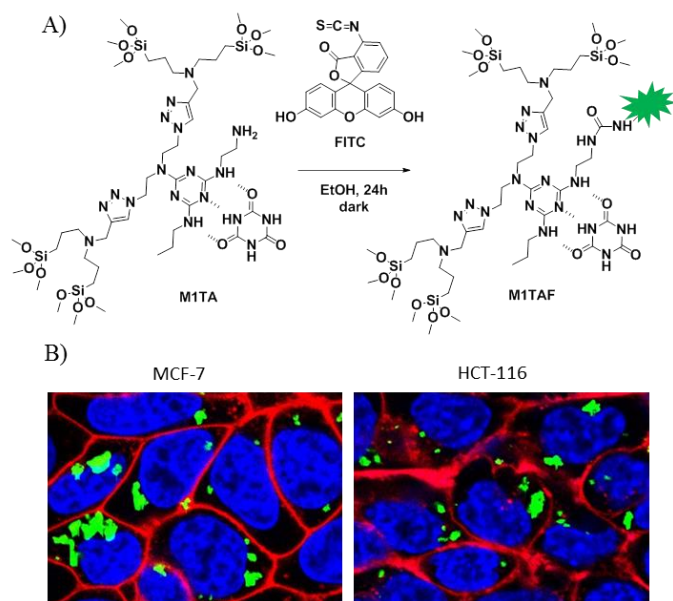


Fig. 9 A) Grafting of FITC on **M1TA** B) Confocal imaging of **M1TAF** in living cancer cells. Human breast (MCF-7) and colorectal (HCT-116) cancer cells are incubated for 24 h with **M1TAF** at a concentration of $20\ \mu\text{g}\cdot\text{mL}^{-1}$. Cell membranes are stained in red with CellMask™ Orange plasma membrane stain, and nuclei in blue with Hoechst 33342.

4. CONCLUSION

Two new tetraethoxysilyl triazine-based precursors (**7** and **8**) bearing a DAD pattern forming H-bonds with CA were synthesized. In contrast to conventional bis-silylated precursors, it was possible to synthesize nano-BS from these new compounds, due to the greater number of hydrolysable triethoxysilyl groups. No CA release was observed from these nano-BS at neutral pH, which would be expected to prevent premature release of the cargo molecule and consequently limit potential side-effects. A parametric study of key process variables, such as reactant concentration, demonstrated that uniform nanoparticles with diameters of $\sim 300\ \text{nm}$ could be readily prepared. Following post-grafting of FITC onto the surface of the nanoparticles, internalization of the nano-BS was clearly demonstrated in both human breast and colorectal cancer cells by fluorescence using confocal microscopy. Work is now underway to further optimize the size of the nanoparticles and to replace CA by more efficacious drugs such as Fluorouracil derivatives, bearing the ADA pattern. In addition to chemotherapy, imaging and also active cell targeting will be examined.

Compliance with ethical standards

Conflict of interest The authors declare that they have no competing interests.

5. REFERENCES

1. Shea KJ, Loy DA, Webster OW (1989) Aryl-bridged polysilsesquioxanes—new microporous materials. *Chemistry of Materials* 1 (6):572-574. doi:10.1021/cm00006a003
2. Corriu RJP, Moreau JJE, Thepot P, Wong Chi Man M (1992) New mixed organic-inorganic polymers: hydrolysis and polycondensation of bis(trimethoxysilyl)organometallic precursors. *Chemistry of Materials* 4 (6):1217-1224. doi:10.1021/cm00024a020
3. Sanchez C, Ribot F (1994) Design of hybrid organic-inorganic materials synthesized via sol-gel chemistry. *New Journal of Chemistry* 18 (10):1007-1047
4. Shea K, Moreau J, Loy D, Corriu R, Boury B, Gomez-Romero P, Sanchez C (2004) Functional hybrid materials. Edited by
5. Elias X, Pleixats R, Wong Chi Man M, Moreau JJ (2006) Hybrid-Bridged Silsesquioxane as Recyclable Metathesis Catalyst Derived from a Bis-Silylated Hoveyda-Type Ligand. *Advanced Synthesis & Catalysis* 348 (6):751-762
6. Monge-Marcet A, Pleixats R, Cattoën X, Wong Chi Man M (2013) Catalytic applications of recyclable silica immobilized NHC–ruthenium complexes. *Tetrahedron* 69 (1):341-348. doi:https://doi.org/10.1016/j.tet.2012.10.023
7. Ferré M, Pleixats R, Wong Chi Man M, Cattoën X (2016) Recyclable organocatalysts based on hybrid silicas. *Green Chemistry* 18 (4):881-922
8. Ferré M, Cattoën X, Wong Chi Man M, Pleixats R (2016) Sol–Gel Immobilized N-Heterocyclic Carbene Gold Complex as a Recyclable Catalyst for the Rearrangement of Allylic Esters and the Cycloisomerization of γ -Alkynoic Acids. *ChemCatChem* 8 (17):2824-2831
9. Graffion J, Cattoën X, Freitas VT, Ferreira RA, Wong Chi Man M, Carlos LD (2012) Engineering of metal-free bipyridine-based bridged silsesquioxanes for sustainable solid-state lighting. *Journal of Materials Chemistry* 22 (14):6711-6715
10. Freitas VnT, Fu L, Cojocariu AM, Cattoën X, Bartlett JR, Le Parc R, Bantignies J-L, Wong Chi Man M, André PS, Ferreira RA (2015) Eu³⁺-based bridged silsesquioxanes for transparent luminescent solar concentrators. *ACS Applied Materials & Interfaces* 7 (16):8770-8778
11. Bourg S, Broudic J-C, Conocar O, Moreau JJ, Meyer D, Wong Chi Man M (2001) Tailoring of organically modified silicas for the solid–liquid extraction of actinides. *Chemistry of Materials* 13 (2):491-499
12. Meyer DJ, Bourg S, Conocar O, Broudic J-C, Moreau JJ, Wong Chi Man M (2007) Extraction of plutonium and americium using silica hybrid materials. *Comptes Rendus Chimie* 10 (10):1001-1009
13. Bhatia RB, Brinker CJ, Gupta AK, Singh AK (2000) Aqueous sol–gel process for protein encapsulation. *Chemistry of Materials* 12 (8):2434-2441
14. Barbe C, Bartlett J, Kong L, Finnie K, Lin HQ, Larkin M, Calleja S, Bush A, Calleja G (2004) Silica particles: a novel drug-delivery system. *Advanced Materials* 16 (21):1959-1966
15. Avnir D, Coradin T, Lev O, Livage J (2006) Recent bio-applications of sol–gel materials. *Journal of Materials Chemistry* 16 (11):1013-1030
16. Chevalier P, Corriu RJ, Delord P, Moreau JJ, Wong Chi Man M (1998) Design of porous silica from hybrid organic–inorganic precursors. *New Journal of Chemistry* 22 (5):423-433
17. Boury B, Chevalier P, Corriu RJ, Delord P, Moreau JJ, Wong Chi Man M (1999) Hybrid Organic–Inorganic Xerogel Access to Meso- and Microporous Silica by Thermal and Chemical Treatment. *Chemistry of Materials* 11 (2):281-291
18. Asefa T, MacLachlan MJ, Coombs N, Ozin GA (1999) Periodic mesoporous organosilicas with organic groups inside the channel walls. *Nature* 402 (6764):867-871. doi:http://www.nature.com/nature/journal/v402/n6764/supinfo/402867a0_S1.html
19. Inagaki S, Guan S, Fukushima Y, Ohsuna T, Terasaki O (1999) Novel Mesoporous Materials with a Uniform Distribution of Organic Groups and Inorganic Oxide in Their Frameworks. *Journal of the American Chemical Society* 121 (41):9611-9614. doi:10.1021/ja9916658
20. Urata C, Yamada H, Wakabayashi R, Aoyama Y, Hirose S, Arai S, Takeoka S, Yamauchi Y, Kuroda K (2011) Aqueous colloidal mesoporous nanoparticles with ethylene-bridged silsesquioxane

- frameworks. *Journal of the American Chemical Society* 133 (21):8102-8105
21. Li X, Zhou L, Wei Y, El-Toni AM, Zhang F, Zhao D (2014) Anisotropic growth-induced synthesis of dual-compartment Janus mesoporous silica nanoparticles for bimodal triggered drugs delivery. *Journal of the American Chemical Society* 136 (42):15086-15092
22. Croissant JG, Cattoën X, Wong Chi Man M, Durand J-O, Khashab NM (2015) Syntheses and applications of periodic mesoporous organosilica nanoparticles. *Nanoscale* 7 (48):20318-20334
23. Croissant J, Cattoën X, Wong Chi Man M, Dieudonné P, Charnay C, Raehm L, Durand JO (2015) One-Pot Construction of Multipodal Hybrid Periodic Mesoporous Organosilica Nanoparticles with Crystal-Like Architectures. *Advanced Materials* 27 (1):145-149
24. Chen Y, Shi J (2016) Chemistry of mesoporous organosilica in nanotechnology: Molecularly organic-inorganic hybridization into frameworks. *Advanced Materials* 28 (17):3235-3272
25. Giret S, Wong Chi Man M, Carcel C (2015) Mesoporous-Silica-Functionalized Nanoparticles for Drug Delivery. *Chemistry – A European Journal* 21 (40):13850-13865. doi:10.1002/chem.201500578
26. Lin CXC, Qiao SZ, Yu CZ, Ismadji S, Lu GQM (2009) Periodic mesoporous silica and organosilica with controlled morphologies as carriers for drug release. *Microporous and Mesoporous Materials* 117 (1):213-219
27. Vathiyam R, Wondimu E, Das S, Zhang C, Hayes S, Tao Z, Asefa T (2011) Improving the adsorption and release capacity of organic-functionalized mesoporous materials to drug molecules with temperature and synthetic methods. *The Journal of Physical Chemistry C* 115 (27):13135-13150
28. Moorthy MS, Park S-S, Fuping D, Hong S-H, Selvaraj M, Ha C-S (2012) Step-up synthesis of amidoxime-functionalised periodic mesoporous organosilicas with an amphoteric ligand in the framework for drug delivery. *Journal of Materials Chemistry* 22 (18):9100-9108
29. Yang Y, Bernardi S, Song H, Zhang J, Yu M, Reid JC, Strounina E, Searles DJ, Yu C (2016) Anion assisted synthesis of large pore hollow dendritic mesoporous organosilica nanoparticles: understanding the composition gradient. *Chemistry of Materials* 28 (3):704-707
30. Yang Y, Lu Y, Abbaraju PL, Zhang J, Zhang M, Xiang G, Yu C (2017) Multi-shelled Dendritic Mesoporous Organosilica Hollow Spheres: Roles of Composition and Architecture in Cancer Immunotherapy. *Angewandte Chemie* (129):8566-8570
31. Du X, Li X, Xiong L, Zhang X, Kleitz F, Qiao SZ (2016) Mesoporous silica nanoparticles with organo-bridged silsesquioxane framework as innovative platforms for bioimaging and therapeutic agent delivery. *Biomaterials* 91 (Supplement C):90-127. doi:https://doi.org/10.1016/j.biomaterials.2016.03.019
32. Mizoshita N, Tani T, Shinokubo H, Inagaki S (2012) Mesoporous Organosilica Hybrids Consisting of Silica-Wrapped π - π Stacking Columns. *Angewandte Chemie International Edition* 51 (5):1156-1160. doi:10.1002/anie.201105394
33. Giret S, Théron C, Gallud A, Maynadier M, Gary-Bobo M, Garcia M, Wong Chi Man M, Carcel C (2013) A Designed 5-Fluorouracil-Based Bridged Silsesquioxane as an Autonomous Acid-Triggered Drug-Delivery System. *Chemistry – A European Journal* 19 (38):12806-12814. doi:10.1002/chem.201301081
34. Fertier L, Théron C, Carcel C, Trens P, Wong Chi Man M (2011) pH-Responsive Bridged Silsesquioxane. *Chemistry of Materials* 23 (8):2100-2106. doi:10.1021/cm103327y
35. Croissant J, Maynadier M, Mongin O, Hugues V, Blanchard-Desce M, Chaix A, Cattoën X, Wong Chi Man M, Gallud A, Gary-Bobo M (2015) Enhanced Two-Photon Fluorescence Imaging and Therapy of Cancer Cells via Gold@ Bridged Silsesquioxane Nanoparticles. *Small* 11 (3):295-299
36. Maggini L, Cabrera I, Ruiz-Carretero A, Prasetyanto EA, Robinet E, De Cola L (2016) Breakable mesoporous silica nanoparticles for targeted drug delivery. *Nanoscale* 8 (13):7240-7247
37. Mauriello-Jimenez C, Henry M, Aggad D, Raehm L, Cattoën X, Wong Chi Man M, Charnay C, Alpugan S, Ahsen V, Tarakci DK (2017) Porphyrin-or phthalocyanine-bridged silsesquioxane nanoparticles for two-photon photodynamic therapy or photoacoustic imaging. *Nanoscale* 9 (43):16622-16626
38. Croissant JG, Mauriello-Jimenez C, Maynadier M, Cattoën X, Wong Chi Man M, Raehm L, Mongin O, Blanchard-Desce M, Garcia M, Gary-Bobo M (2015) Synthesis of disulfide-based biodegradable bridged silsesquioxane nanoparticles for two-photon imaging and therapy of cancer cells. *Chemical Communications* 51 (61):12324-12327
39. Mauriello-Jimenez C, Croissant J, Maynadier M, Cattoën X, Wong Chi Man M, Vergnaud J, Chaleix V, Sol V, Garcia M, Gary-Bobo M (2015) Porphyrin-functionalized mesoporous organosilica nanoparticles for two-photon imaging of cancer cells and drug delivery. *Journal of Materials Chemistry B* 3 (18):3681-3684
40. Gao Y, Chen L, Zhang Z, Gu W, Li Y (2010) Linear Cationic Click Polymer for Gene Delivery: Synthesis, Biocompatibility, and In Vitro Transfection. *Biomacromolecules* 11 (11):3102-3111. doi:10.1021/bm100906m
41. Bürglová K, Noureddine A, Hodačová J, Toquer G, Cattoën X, Wong Chi Man M (2014) A general method for preparing bridged organosilanes with pendant functional groups and functional mesoporous organosilicas. *Chemistry-A European Journal* 20 (33):10371-10382
42. Noureddine A, Trens P, Toquer G, Cattoën X, Wong Chi Man M (2014) Tailoring the Hydrophilic/Lipophilic Balance of Clickable Mesoporous Organosilicas by the Copper-Catalyzed Azide-Alkyne Cycloaddition Click-Functionalization. *Langmuir* 30 (41):12297-12305